Science of the Total Environment 648 (2019) 25–32

Contents lists available at ScienceDirect

Science of the Total Environment

journal homepage: www.elsevier.com/locate/scitotenv

Scoping studies to establish the capability and utility of a real-time bioaerosol sensor to characterise emissions from environmental sources

Zaheer Ahmad Nasir [a,*], Enda Hayes [b], Ben Williams [b], Toni Gladding [c], Catherine Rolph [c], Shagun Khera [d], Simon Jackson [d], Allan Bennett [e], Samuel Collins [e], Simon Parks [e], Alexis Attwood [f], Robert P. Kinnersley [g], Kerry Walsh [g], Sonia Garcia Alcega [a], Simon J.T. Pollard [a], Gill Drew [a], Frederic Coulon [a], Sean Tyrrel [a]

[a] School of Water, Energy and Environment, Cranfield University, Cranfield MK43 0AL, UK
[b] Air Quality Management Resource Centre, Faculty of Environment and Technology, University of the West of England, Bristol BS16 1QY, UK
[c] STEM Faculty, Open University, Walton Hall, MK6 7AA, UK
[d] School of Biomedical and Healthcare Sciences, Plymouth University, Drake Circus, Plymouth PL4 8AA, UK
[e] Biosafety, Air and Water Microbiology Group, National Infection Service, Public Health England, Salisbury SP4 0JG, UK
[f] Droplet Measurement Technologies, 2400 Trade Centre Avenue, Longmont, CO 80503, United States of America
[g] Environment Agency, Evidence Directorate, Deanery Road, Bristol BS1 5AH, UK

HIGHLIGHTS

- First real world evaluation of a novel dual wavelength excitation multiple fluorescence band bioaerosol sensor
- High variability in nature and magnitude of emissions at contrasting sites
- Highly resolved emission intensity measurements provide additional spectral information in comparison to existing devices.
- Differences in emission spectra from different sites at smaller and lager wavelengths than maxima

GRAPHICAL ABSTRACT

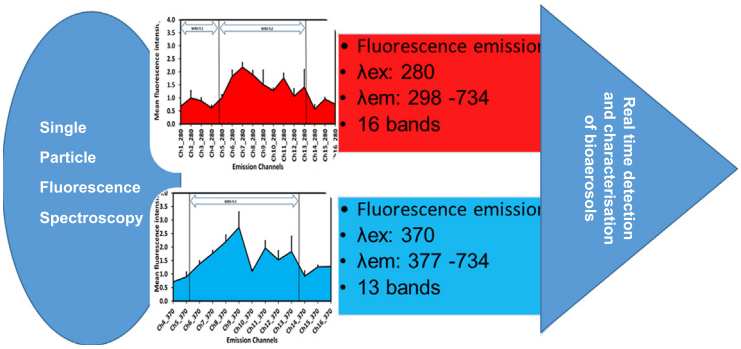

ARTICLE INFO

Article history:
Received 14 April 2018
Received in revised form 8 August 2018
Accepted 9 August 2018
Available online 09 August 2018

Editor: D. Barcelo

Keywords:
Real-time monitoring
Bioaerosols
Emissions characterisation
Fluorescence spectra

ABSTRACT

A novel dual excitation wavelength based bioaerosol sensor with multiple fluorescence bands called Spectral Intensity Bioaerosol Sensor (SIBS) has been assessed across five contrasting outdoor environments. The mean concentrations of total and fluorescent particles across the sites were highly variable being the highest at the agricultural farm (2.6 cm^{-3} and 0.48 cm^{-3}, respectively) and the composting site (2.32 cm^{-3} and 0.46 cm^{-3}, respectively) and the lowest at the dairy farm (1.03 cm^{-3} and 0.24 cm^{-3}, respectively) and the sewage treatment works (1.03 cm^{-3} and 0.25 cm^{-3}, respectively). In contrast, the number-weighted fluorescent fraction was lowest at the agricultural site (0.18) in comparison to the other sites indicating high variability in nature and magnitude of emissions from environmental sources. The fluorescence emissions data demonstrated that the spectra at different sites were multimodal with intensity differences largely at wavelengths located in secondary emission peaks for λex 280 and λex 370. This finding suggests differences in the molecular composition of emissions at these sites which can help to identify distinct fluorescence signature of different environmental sources. Overall this study demonstrated that SIBS provides additional spectral information compared to existing instruments and capability to resolve spectrally integrated signals from relevant biological fluorophores could improve selectivity and thus enhance discrimination and classification strategies for real-time characterisation of bioaerosols

* Corresponding author.
E-mail address: z.a.nasar@cranfield.ac.uk (Z.A. Nasir).

https://doi.org/10.1016/j.scitotenv.2018.08.120

from environmental sources. However, detailed lab-based measurements in conjunction with real-world studies and improved numerical methods are required to optimise and validate these highly resolved spectral signatures with respect to the diverse atmospherically relevant biological fluorophores.

1. Introduction

Bioaerosols, airborne particles of biological origin, come from both natural and anthropogenic sources and have potential impacts on global (climatic processes), regional (ambient microbiome) and local (public health) scales. Along with investigations on their climate interaction and long-distance transport, the public health impact of bioaerosols has received significant attention due to a growth in existing and emerging sources of bioaerosols such as waste management operations and intensive agriculture facilities, as well as the resultant human risk of exposure in occupational settings and the wider community (Douglas et al., 2016; Jahne et al., 2016; Madsen et al., 2016; Borlée et al., 2015; Pearson et al., 2015; Walser et al., 2015; Pankhurst et al., 2012; van der Hoek et al., 2012; O'Connor et al., 2010; Bünger et al., 2007; Sykes et al., 2007; Taha et al., 2007, 2006, 2005). Hence there has been increasing interest in detection and characterisation of bioaerosols emissions from various environmental sources. Over the last decade there have been growing efforts to advance methods for detecting the abundance, distribution, diversity and properties of bioaerosols, as well as their environmental impact across different temporal and spatial scales (Anderson et al., 2016; Jahne et al., 2016; Mazar et al., 2016; Pearce et al., 2016; Sialve et al., 2015; O'Connor et al., 2015; Morris et al., 2014; Pankhurst et al., 2012; Vestlund et al., 2014; Sun and Ariya, 2006; Taha et al., 2005).

At present, there are diverse sampling methods with a range of post-collection analyses (culture and non-culture based) for identification and quantification of bioaerosols or their derivatives. However, these are labour intensive and offer snapshot data with low temporal resolution. The capability to quantify the magnitude and spatiotemporal characterisation of bioaerosols emissions from different environmental sources is critical to gauge temporal emission factors and their determinants, developing emission inventories or exposure estimates, advancing forecast modelling and proposing evidence-based management strategies. Recent technological developments have led to the application of a variety of techniques in detection and characterisation of atmospheric bioaerosols from various sources including; electron microscopy epifluorescence microscopy, elastic scattering, laser-breakdown (LIBs), X-ray fluorescence spectroscopy, infrared (IR) absorption, Raman spectroscopy, laser/light-induced fluorescence (LIF), biochemical analysis (e.g., sequencing of DNA or RNA), chromatography, mass spectrometry and nuclear magnetic resonance (NMR) (Pan, 2015; Pöhlker et al., 2012). Among these techniques, fluorescence spectroscopy has shown promising potential for detecting and broadly classifying bioaerosols in real time (Pan, 2015). Instruments based on LIF and/or elastic scattering have recently become commercially available and have shown their capability to detect bioaerosols in real-time over a range of ambient environments and sources: urban/suburban/background (Wei et al., 2016; Yu et al., 2016; Saari et al., 2015; O'Connor et al., 2014; Toprak and Schnaiter, 2013; Gabey et al., 2011; Huffman et al., 2010), dust storms (Hallar et al., 2011), tropical rainforests (Huffman et al., 2012; Gabey et al., 2011; Gabey et al., 2010), high-altitudes (Crawford et al., 2016; Ziemba et al., 2016; Gabey et al., 2013), boreal forest environments (Schumacher et al., 2013; Huffman et al., 2013), industrial processes (O'Connor et al., 2015; Li et al., 2016) and in the atmospheric boundary layer (Perring et al., 2015).

A fairly large body of research is available on lab-based excitation emission characteristics for a range of biologically relevant fluorophores (Hernandez et al., 2016; Pöhlker et al., 2012; Pan et al., 2010; Hill et al., 2009). However, in the natural environment, bioaerosols are part of a complex mixture differing significantly from lab-based studies. The diversity of biological and non-biological interfering compounds significantly hampers the selectivity of LIF based bioaerosol detectors. The most advanced approach is the use of elastic scattering and dual wavelength excitation of single particles and measurement of spectrally resolved fluorescence along with size and shape in real time. One limitation of existing commercially available LIF based detectors is their broad emission detection bands that make it difficult to classify or discriminate between different types of bioaerosols (Pöhlker et al., 2012). Recently a novel LIF based sensor with highly resolved fluorescence intensity measurements (Spectral Intensity Bioaerosol Sensor (SIBS) has been developed by Droplet Measurement Technologies Inc. (Longmont, USA). The SIBS is an expansion of the Wideband Integrated Bioaerosol Sensor (WIBS) which was developed by the University of Hertfordshire (Kaye et al., 2005). The WIBS uses two excitation wavelengths ($\lambda ex = 280$ nm and 370 nm) and measures fluorescence in three emissions (λem) bands as follows: FL1: $\lambda ex = 280$ nm, λem ~ 310–400 nm, FL2: $\lambda ex = 280$ nm, λem ~ 420–650 nm, and FL3: $\lambda ex = 370$ nm, λem ~ 420–650 nm. In contrast, fluorescence emission is measured by the SIBS across 16 wavelength bands from $\lambda em = 288$–735 nm for two excitation wavelengths ($\lambda ex =$ 280 nm and 370 nm) providing greater spectral resolution in the emission signal from a bioaerosol. In this paper the capability and utility of SIBS was evaluated at contrasting land uses to demonstrate the novel capability of the SIBS to record highly resolved emission spectra. To the best of the authors' knowledge, this is the first study of this kind where SIBS has been employed and tested in a range of real-world emission scenarios.

2. Materials and methods

2.1. Sampling sites and design

Five contrasting outdoor environments were selected for this study including an agricultural farm, a dairy farm, an urban background site, a sewage treatment works and green waste composting facility (Table 1). All the sites are in the United Kingdom and have been anonymised except for the urban background (Cranfield University). Three measurements were made during daytime at a height of 1 m and site activity logs were kept during each sampling period. Table 1 provides a general description of the sites and sampling strategy.

2.2. Instrumentation

Continuous real-time measurements were made with a SIBS comprising of a central optical chamber, a continuous-wave 785 nm diode laser through which particles pass and scatter light, a quadrant photomultiplier tube (PMT) placed to measure the forward scattered light from which the particle shape is derived, an avalanche photodiode (APD) for particle detection and sizing, two pulsed xenon UV sources emitting sequentially at two different wavebands (280 and 370 nm), and a 16 channel photomultiplier spectrometer. A dichroic mirror directs the scattered light to the APD, and the fluorescence emission, 288–720 nm is collected by the two chamber mirrors and delivered through the mirror aperture onto a dichroic beam-splitter that passes the 288–720 nm emissions directly to the spectrometer where it is resolved into 16 channels (Table 2).

Table 1
Summary details of sampling sites.

Site	Description	Sampling strategy
Agricultural farm	• A large area with arable land mainly cultivated with wheat and rape • distant from main roads and wood land	• Sampling was conducted at the edge of the agriculture field. • 3 repeated measurements of 2 h duration each. • Sampling in April and May 2016
Dairy farm	• A small 45 acre farm with 22 cows and followers, free range pigs and hens. • Surrounded by arable fields and a small horse riding stable	• Sampling was conducted adjacent to a cowshed. • 3 repeated measurements of ~ 4 h each • Sampling in May 2016
Urban background	• A grassed area with mature trees nearby • Surrounded by university campus buildings.	• Sampling was conducted at grass plot at the Cranfield University. • 3 repeated measurements for 3–3.5 h each • Sampling in February–March 2016
Sewage treatment works	• A trickling filter based sewage treatment plant which treats wastewater and storm drains with a daily capacity of 450 m^3. • Surrounded by agricultural fields and wood land	• Sampling between the primary trickling filter beds and the settling tank. • 3 repeated measurements of 3–3.5 h duration. • Sampling in February and April 2016
Green waste composting	• Approximately 15,000 t per year of organic waste products such as green garden waste (trees, grass clippings, hedge trimmings etc.), fruit & vegetable waste, straw, stable waste paper and card are processed. • Operational area is approximately 6 ha which sits within a farm of about 22 ha. • Surrounded by arable fields, crops between seedlings and flowering stage	• Downwind sampling at 90 and 136 m (depending on wind direction) • 3 repeated measurements of ~4 h each • Sampling in March, May and October 2016

Thus, for each fluorescing particle, a 2 × 16 excitation-emission matrix is recorded along with an estimate of particle size and shape (asphericity). The SIBS used in this study has sample flow rate of 0.3 l/min and derives the equivalent optical diameter (EOD) and asphericity, in the size range from 0.4–7 μm, along with the excitation-emission matrix of single particles. Particle size calibration was carried out by Droplet Measurement Technologies, USA, prior to the sampling campaign using standard monodisperse polystyrene latex microspheres with a refractive index of 1.58. Prior to the field deployment, the performance tests on sizing and spectral response were also conducted in-house by using 2 μm non-fluorescent polymer microspheres and green fluorescent polymer microspheres (Figs. 1, 2 and 3 supplementary data).

Table 2
Fluorescence measurement channels (Ch) and wavelength ranges (nm).

Channel	Lower wavelength	Upper wavelength
1	298.2	316.4
2	316.4	344.8
3	344.9	362.5
4	377.5	401.5
5	401.5	429.7
6	430.2	457.5
7	456.7	485.6
8	486.0	514.0
9	514.1	542.0
10	542.0	569.8
11	569.9	597.6
12	597.6	625.2
13	625.3	652.8
14	652.8	680.2
15	680.3	707.5
16	707.5	734.7

2.3. Data analysis

The SIBS stores single particle data and these were imported into a data analysis toolkit for offline data processing. The single particle data files were analysed by choosing an averaging interval of 60 s from 0.5–0.7 μm. During operation, the SIBS always records a background fluorescence signal due to some flash lamp light reaching the monochromator and photomultiplier assembly (bleed-through). To quantify the level of this signal the SIBS is routinely run in a "Forced Trigger" mode such that the sample pump is turned off and the Xenon lamps are set to fire at 150 ms intervals. A minimum of 5 m forced trigger data was collected prior to the start of each measurement at a site. This was used to define a lower fluorescence threshold in order to calculate number concentration of fluorescent particles such that particles that fluoresce with lower intensity, and might be non-bioaerosols, are removed from the analysis. We used a single lower fluorescence threshold value (20) calculated from mean forced trigger values of all the channels + 3 × mean SD values of all the channels. The data on forced trigger measurements are presented in Fig. 4 (Supplementary data). Additionally, during the recharge of flash lamps, there will be no fluorescent measurements and some particles may not be flashed. This leads to three categories of particles: total particles, excited particles and fluorescent particles. Hence, the concentration of fluorescent particles was calculated using Eq. (1) to correct for particles missed by the flashlamp.

$$\text{Fluorescent concentration } (\text{cm}^{-3}) = (\text{F}/\text{E})^{*}\,\text{T} \quad (1)$$

where T = Total particles (cm^{-3}), E = Excited particles (cm^{-3}) and F = Fluorescent particles (cm^{-3}) (based on the fluorescence threshold calculated from forced trigger data.

For the analysis of fluorescence spectra at different sites, a mid-sampling point single particle data file during each repeated measurement at each site was selected except green waste composting where a data file during turning was selected. All the unexcited particles were excluded from the selected data files to carry out emission intensity analysis. The sample size for analysis of fluorescence spectra at different sites is shown in Table 3.

For each particle sample data file from a site, mean forced trigger emission intensities values were subtracted from the particle by particle emission intensity values in corresponding channels followed by the calculation of mean fluorescence intensity across the emission wavelength bands of the SIBS for two excitation wavelengths. Thus, three fluorescence spectra were obtained for each site. Finally, from these three individual emission spectra for a site, a mean fluorescence spectrum along with standard deviation value in each channel was computed for all the sites.

3. Results and discussion

3.1. Number concentrations

The number concentrations of the total and fluorescing particles (calculated using Eq. (1)), along with the number ratios of fluorescent to total concentrations are listed in Table 4. The highest number concentrations for total (NT = 2.6 cm^{-3}) and fluorescent particles (NF = 0.48 cm^{-3}) were recorded at the agricultural farm and green waste composting (NT = 2.32 cm^{-3}, NF = 0.46 cm^{-3}). In contrast, mean number fluorescent fraction was lowest at the agricultural site (0.18) than other sites and less variable.

The coefficient of variation (the ratio of the standard deviation to the mean) revealed large variability in number concentration of both the total and fluorescent particles over the three measurements periods at

Table 3
Sample size of particles for the analysis of fluorescence intensity across different wavelength bands at each site.

Sites	Sampling 1 Number of particles	Sampling 2 Number of particles	Sampling 3 Number of particles	Total Number of particles
Agricultural farm	16,329	12,611	20,213	49,153
Dairy farm	26,699	12,883	18,928	58,510
Urban background	25,830	19,744	28,035	73,609
Sewage treatment works	14,949	24,479	24,839	64,267
Green waste composting	24,412	15,046	4045	43,503

the different sites, in particular at green waste composting and sewage treatment works (Table 3). This reflects significant impact of time-dependent site-specific factors on emissions, especially for industrial sources, and highlights the shortcomings of snapshot infrequent sampling to quantify magnitude and nature of bioaerosols emissions from environmental sources. Studies using the WIBS in different ambient environments have reported similar variability in number concentrations of biological particles related to location and season. Gabey et al. (2010, 2011 and 2013) conducted studies in urban (winter), tropical and high altitude environments and observed bioaerosol number concentrations of 0.1 cm^{-3}, 0.2–1.5 cm^{-3} and 0.1 cm^{-3}, respectively. Similarly, number concentrations of fluorescent aerosol particles in an urban area reported by Toprak and Schnaiter (2013) were variable across the seasons, being highest (0.046 cm^{-3}) in summer and lowest in winter (0.019 cm^{-3}). In the context of number concentrations of biological particles from industrial emissions, a recent study conducted using the WIBS at a green composting site showed a range of 0.10–0.30 cm^{-3} during light and heavy workloads (O'Connor et al., 2015). By comparison, in our study, the average number concentration of fluorescent particles at composting sites was 0.46 cm^{-3}.

In terms of number weighted fluorescent fraction, the mean at different sites ranged from 0.18 (agricultural) to 0.25 (Urban background) with the highest variability across different measurements at the composting site (CV = 21%) again highlighting the impact of various spatio-temporal factors on bioaerosol emissions. Atmospheric bioaerosols concentrations have been reported to be highly variable and can be affected by biological activity and meteorological factors (Toprak and Schnaiter, 2013; Bauer et al., 2008). Toprak and Schnaiter (2013) recently reported that number concentration fractions of fluorescent biological aerosol particles at an urban site during winter were from 0.0043–0.18. A similar study by O'Connor et al. (2015) at a composting site, with measurements using the WIBS, found that more than half of the total particles were fluorescent during heavy site activity. In the present study, fluorescent particles represented up to 0.44 of total particles at ~ 100 m downwind of activity at the composting site. The observed differences are likely due to variability in microclimate, sampling characteristics and different size ranges (0.8–16 μm for Toprak and Schnaiter (2013) and 0.69 - ~ 13 μm for O'Connor et al. (2015)). No direct comparison can be made between the present investigation and these studies due to differences in the detectable range of particle size and specific environmental/sampling characteristics. Nonetheless, these findings show the impact of various sources/activities on temporal bioaerosols emissions loadings and the capability of real-time monitoring to identify sources and elucidate their level of contribution to atmospheric bioaerosols.

Table 4
Summary of particles concentrations at each site (number of measurement $n = 3$).

		Number concentration		Ratio
		NT(cm^{-3})	NF(cm^{-3})	NF/NT
Agricultural farm	Average	2.6	0.48	0.18
	CV (%)	16	24	7
Dairy farm	Average	1.03	0.24	0.24
	CV (%)	26	25	5
Urban background	Average	1.17	0.29	0.25
	CV (%)	17	11	6
Sewage treatment works	Average	1.03	0.25	0.24
	CV (%)	43	40	3
Green waste composting	Average	2.32	0.46	0.21
	CV (%)	75	56	21

NT = Number of total Particles, NF = Number of fluorescent particles, CV = Coefficient of variation.

3.2. Fluorescence spectra from different environmental sources

Fluorescence intensity across emission wavelength bands of the SIBS for the two excitation wavelengths (280 nm and 370 nm) for all the sites is illustrated in Figs. 1 and 2.

As a first approach for qualitative description, emission spectra at each site are explained in terms of emission zones as a function of wavelength. The 280 nm excitation fluorescence spectra of the agricultural site shows peak fluorescence emission in 456.7–485.6 nm (Ch 7) and 569.9–597.6 nm (Ch 11) along with secondary peaks at 316.4–362.5 nm (Ch 2–3) and 625.3–652.8 nm (Ch 13) and 680–707 nm (Ch15). In contrast, the 370 nm excitation fluorescence spectrum had a sharp peak at 514–542 nm (Ch 9) with secondary peaks at 569.9–652.8 nm (Ch 11–13) and 680–734.7 nm (Ch 15–16). At the dairy farm for both 280 nm and 370 nm excitation, the emission spectra were comparable to the agricultural site with slight differences at 569.9–652.8 nm (Ch 11–13) in secondary emission modes.

The peak emission zone for 280 nm excitation, at urban background site, was centred at 456.7–485.6 nm (Ch 7) with secondary peaks at 316.4–344.8 nm (Ch 2), 542–569.85 (Ch 10), 597.6–625.2 nm (Ch 12) and 680.3–707.5 nm (Ch 15). Similarly, at 370 nm excitation, emission spectrum was multimodal with peaks at 514–542 nm (Ch 9), 597.6–625.2 nm (Ch 12) and 680.3–707.5 nm (Ch 15), respectively. The samples from sewage treatment works had a broad emission peak at 430.2–514 nm (Ch 6–8) followed by a secondary peak at 597.6–625.2 nm (Ch 12) and 680.3–707.5 nm (Ch 15), for 280 nm excitation. The emission spectrum for 370 nm excitation had peaks at 514–542 nm (Ch 9), 597.6–652.8 nm (Ch 12–13) and 680.3–707.5 nm (Ch 15).

For the green waste composting, the spectrum for 280 nm excitation was multimodal and characterised by a fluorescence maximum at 430.2–485.6 nm (Ch 6–7) with secondary peaks at 316.4–344.8 nm (Ch 2), 486–542 nm (Ch 8–9) and 597.6–625.2 nm (Ch 12). In contrast, for the 370 nm excitation, the spectrum peaked at 514.1–542 (Ch 9) with shoulder peaks at 430.2–457.5 nm (Ch 6), 597.6–625.2 nm (Ch 12) and 680.3–734.7 nm (Ch 15–16).

In broader terms differences were found in the general shapes of the emissions spectra at different sites, in particular, the magnitude and wavelength of the secondary peaks at smaller and larger wavelengths than the maxima. Nevertheless, the assignment of fluorescence to specific biological fluorophores within atmospheric particles is challenging. Currently, a tangible explanation of the molecular origin of fluorescence in different channels from particle population at these sites is unavailable but based on existing findings on LIF spectra of atmospherically relevant biological fluorophores assignments can be deduced. This can help to understand the underlying determinants of these differences and thus identifying distinct fluorescence signature of different environmental sources. The available literature on excitation and emission

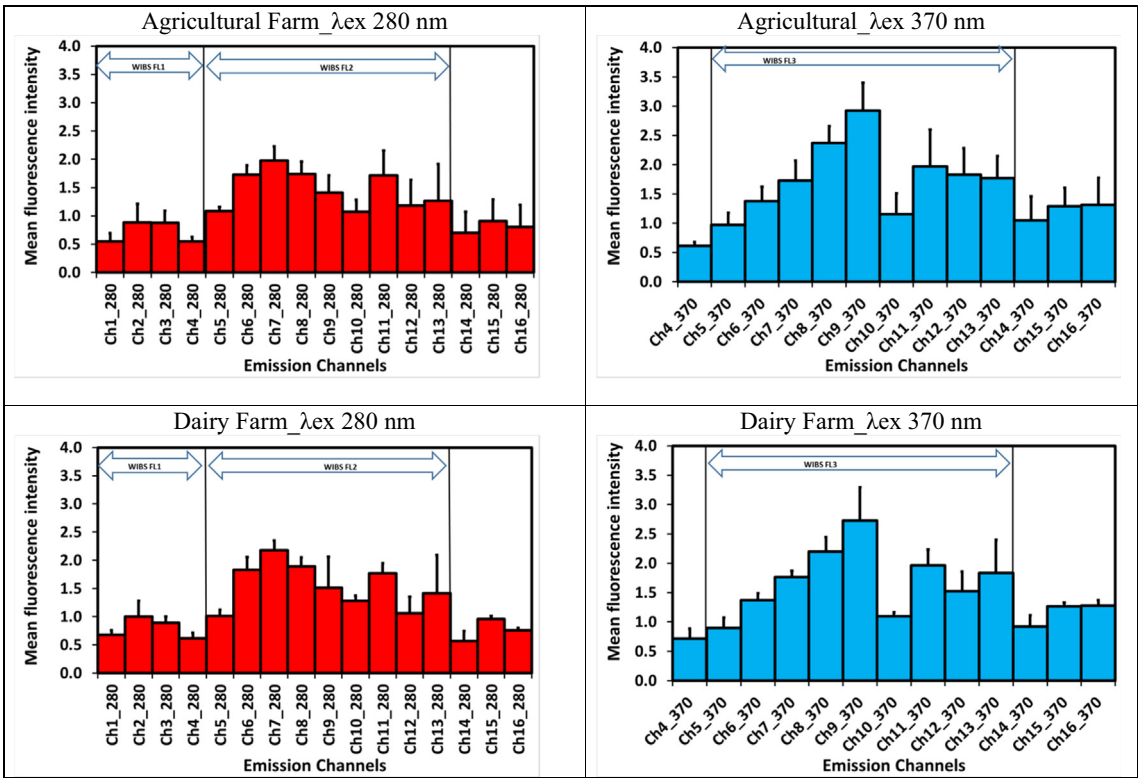

Fig. 1. Mean fluorescence spectra for two excitation wavelengths at the agricultural and dairy farm. Bars = standard deviation.

matrix spectra of a variety of biological fluorophores can help to offer insights about the composition of particles (Hernandez et al., 2016; Pöhlker et al., 2012; Pan et al., 2010; Hill et al., 2009). According to the available data with respect to atmospherically relevant biological fluorophores, the emission wavelength from 400 to 500 nm is crowded by a number of biological fluorophores and emissions in this zone could originate from a mixed signal from a variety of compounds. In contrast, the emission zone from 500 to 700 is relatively clearer with compounds exhibiting larger Δλ stokes (such as riboflavin, chlorophyll *b*). Whereas, emissions at 300–350 nm are characteristics of amino acids (Phenylalanine, Tyrosine and Tryptophan).

Among the five studied sites different emission zones at λex 280 nm could be assigned to amino acids (e.g. Tyrosine, tryptophan and phenylalanine in Ch 1–3), several coenzymes/cofactors and structural biopolymers (e.g. pyridoxine, cellulose, neopterin, chitin, phenylocoumarin in Ch 4–8), and flavins in Ch 9–10. The potential source of emission in Ch 4–10 (377.5–569.8 nm) for λex 370 could be from diverse coenzymes/cofactors (NADPH, flavins, neopterin, lumazine) and a range of structural biopolymer or their constituents (cellulose, chitin, ferulic acids, phenylocoumarin). The emission in Ch 11–16 (569.9–734.7 nm) could be from secondary metabolites (e.g. Alkaloids, terpenoids) and pigments (e.g. Chlorophyll). However, secondary metabolites and age-related pigments have been reported to have broad emission bands and could contribute in Ch 5–Ch 16 for both λex 280 and λex 370. For example, for λex 250–395 nm, terpenoids from plants and fungi have reported λem in the range of 400–725 nm and lipofuscin has λem in the range of 430–670 nm for λex 260–280 nm and 340–490 nm (Pöhlker et al., 2012).

The primary peaks, for both 280 nm and 370 nm excitation, at different sites was at 430–514 nm (Ch 6–8) and 514.1–542 (Ch 9), respectively. The predominant emission in Ch 6–8 (430–514 nm) is possibly from structural compounds (cellulose (dry), chitin (Dry), lignin (phenylcoumarin), and coenzyme (e.g. Neopterin). While the emission at 514.1–542 (Ch 9) for 370 nm excitation can be assigned to flavins. The secondary peaks for both the excitation wavelengths are centred in Ch 11 (596.9–597.6 nm), Ch 12 (597.6–625.2 nm), Ch 13 (625.3–652.8 nm), and Ch 15–16 (680.3–734.7 nm) of the spectra and relevant biological fluorophore in this region are likely to be from secondary metabolites (e.g. alkaloids, terpenoids) pigments (e.g. chlorophyll, flavonoids, lipofuscin). Lipofuscins are age-related pigments reported to be formed due to oxidative stress and has a wide emission range from blue to red (Roshchina, 2012), whereas emissions in Ch 1–3 (298 – 362 nm) are reported to be from amino acids. The differences in secondary emission peaks at different sites suggest that compounds with weak fluorescence could play a role in selectivity. Although the emission wavelengths with the highest intensity constitute the dominant mode of the spectra the contribution from low emission intensity at a specific wavelength is of value to disentangle the mixed fluorescence singles from a source. This assessment could inform the development of hypotheses on how and why molecular composition varies between particle populations at different sites which can be tested in further experimentations and analysis.

The secondary emission peaks for both λex 280 and λex 370 were variable across sites and centered at lower and larger wavelength than maxima. The observed shift in emission modes at smaller and larger wavelengths than the peaks at different sites could be due to the underlying differences in chemical composition of emissions at these sites. However, in the natural environment, bioaerosols are part of a complex mixture differing significantly from lab-based studies. This diversity of biological and non-biological interfering compounds significantly hampers the selectivity of LIF based bioaerosol detectors. Therefore, assigning a spectral response to the classification of bioaerosols is the biggest challenge due to wide emission bands and overlapping fluorescence signatures. The SIBS tackles this challenge with an improved spectral resolution to elucidate spectrally integrated signals by measuring fluorescence emission spectra in 16 wavelength bands. In the case of the WIBS the three emission bands FL1 (λex = 280 nm, λem ~ 310–400 nm), FL2 (λex = 280 nm, λem ~ 420–650 nm) and FL3 (λex = 370 nm, λem ~ 420–650 nm) will give an integrated signals for a range of fluorophores. Proteins and coenzymes are likely to dominate the emission signal in FL1

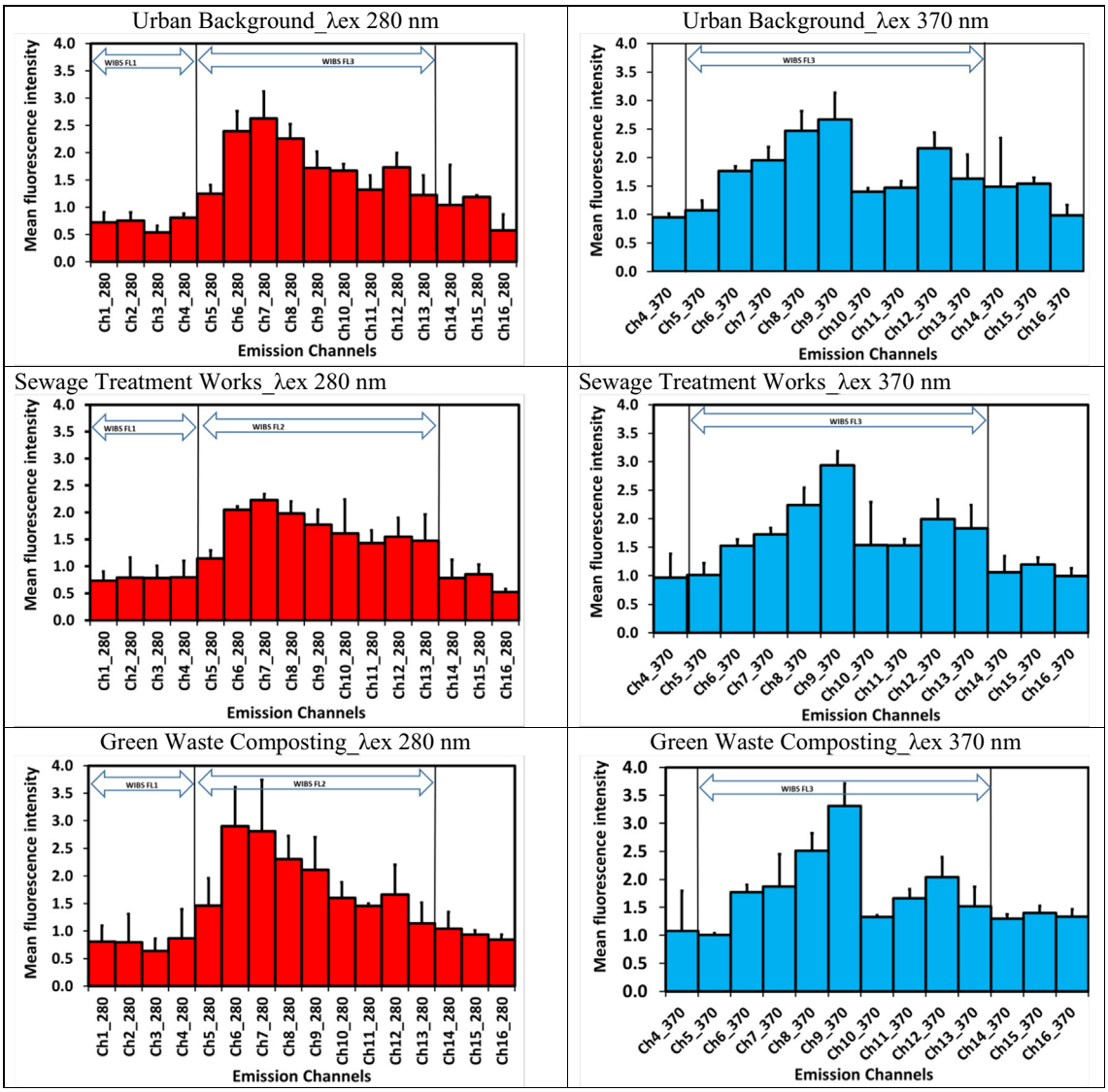

Fig. 2. Mean fluorescence spectra for two excitation wavelengths at the urban background, sewage treatment works and green waste composting. Bars = standard deviation. (For interpretation of the references to colour in this figure legend, the reader is referred to the web version of this article.)

and structural compounds along with certain coenzymes are likely to be detected in FL2. Similarly, the emission spectral region for FL3 can only detect an integrated fluorescence for a range of coenzymes, structural compounds and secondary metabolites. Therefore, offering poor selectivity for a specific biological fluorophore and hence limiting the suitability of these emission bands to discriminate bioaerosols. For instance, the assumption about FL3 emissions as an indicator of metabolic state may not hold true due to the diversity of biological fluorophore emitting in this range. Furthermore, WIBS is unlikely to detect compounds with larger Δλ stokes (chlorophyll or secondary metabolites). In contrast, it can be seen that highly resolved fluorescence intensity measurements by the SIBS provides more detailed spectral information as compared to broad emission bands in the WIBS and that the additional channels in the SIBS are revealing information that is lost in the WIBS (Figs. 1 and 2). However extensive laboratory studies are yet to be performed to offer meaningful interpretations of this additional spectral information in the context of complex ambient aerosol samples. Hence, the above description is an overview of the capability of improved spectral resolution to elucidate spectrally integrated signals from contrasting environmental sources based on lab-based measurements on excitation and emission matrix spectra of the most relevant biological fluorophores.

In terms of particle size of the sample data for fluorescence spectra analysis in Figs. 1 and 2, most of the particles measured at these sites were predominantly of fine size fraction. The mean particle size ranged from 0.59 μm (Sewage treatment works) to 0.87 μm (Green waste composting) with considerable variation at each site (Table 5).

The fluorescence in these size fractions (below 1 μm) could originate from the contribution from cellular fragments or molecular decomposition products of biological material as well as non-biological materials. Further studies are required to address the molecular origin of fluorescence in fine and ultrafine particles in the air and to establish their relevance and implications to characterise bioaerosols

Table 5
Particle size (μm) of sample data for fluorescence spectra analysis at different sites (n = number of particles).

Site	Mean	Minimum	Maximum	Standard deviation
Agricultural farm (n = 49,153)	0.65	0.4	6.77	±0.52
Dairy farm (n = 58,510)	0.61	0.4	6.80	±0.48
Urban background (n = 73,609)	0.67	0.4	6.81	±0.56
Sewage treatment works (n = 64,267)	0.59	0.4	6.81	±0.44
Green waste composting (n = 43,503)	0.87	0.4	6.82	±1.01

emissions. Fluorescence properties of a fluorophore are highly dependent on the molecular environment and this in biological cells or their fragments could be much more dynamic and complex leading to differences in intensity and emission modes in atmospheric bioaerosols in comparison to lab-based studies of pure biological fluorophores (Pan, 2015). Furthermore, atmospheric aerosols from both anthropogenic and natural sources have a range of biological and non-biological fluorescent constituents and therefore emission spectra are characterised by mixed signals from different fluorophores. Non-biological compounds such as secondary organic aerosols, mineral dust and polycyclic aromatic hydrocarbons can cause positive fluorescence measurement artefacts. Consequently, a selective assignment of the molecular origin of fluorescence is not straightforward. Thus differences in emission intensity should be viewed as semi-quantitative and analysed adjunct to overall spectra.

4. Conclusions and future directions

The capability and utility of a novel LIF sensor based on dual-wavelength excitation with highly resolved fluorescence intensity measurements (Spectral Intensity Bioaerosol Sensor (SIBS)) to characterise bioaerosols emissions in real time was evaluated. The number concentration of total and fluorescent particles was highly variable across the sites. Emission spectra from different sites were multimodal with intensity differences at some channels for both excitation wavelengths. It has been demonstrated that highly resolved emission intensity measurements by the SIBS provides additional spectral information in comparison to the WIBS. This demonstrates that SIBS can contribute to overcoming the selectivity challenges to discriminate and classify bioaerosols emissions. However, improved numerical methods and tools are needed to utilise this detailed information to develop discrimination algorithms. Different post detection methods (e.g. principal component analysis, Hierarchical agglomerative cluster analysis, Linear discriminant analysis) have been proposed and used to discriminate biological classes and other interferants (Crawford et al., 2015; Pan, 2015; Robinson et al., 2013; Pan et al., 2010) with data from existing LIF based instruments. These approaches and methodologies are evolving and deemed suitable for SIBS data but are yet to be tested to develop an optimised classification method. However, there is pressing need to conduct lab-based studies with atmospherically relevant biological fluorophores/aerosols in order to build comprehensive SIBS fluorescence spectra library. Such library will greatly contribute to the elucidation of spectrally integrated signals and thus improving measurement selectivity for bioaerosols emissions. At the same time, comparative measurements of SIBS with other biochemical detection methods focusing on various constituents (endotoxin, peptidoglycans, β1–3 glucan, DNA) or metabolites (mVOC) (qPCR, LAL, GC–MS, flow cytometry) and development of improved analysis methods to analyse the complex set of data generated by the SIBS will advance the use of single particle LIF based technique as a powerful analytical tool to characterise bioaerosols emissions from environmental sources.

5. Limitations of the study

The SIBS is a beta version device and the measurements reported in this paper were one of the earliest versions of the SIBS with limited data analysis capability. One of the limitations of this study, for example, is that we used a single fluorescence threshold value to calculate number concentration of fluorescent particles. Ideally, individual lower fluorescence threshold limits for all the channels should be set to derive wavelength based fluorescent particle time series data (channel by channel). The fluorescence spectra analysis, however, is carried out by subtracting mean forced trigger emission intensity values from the particle by particle emission intensity values in corresponding channels. Nonetheless, the results should be interpreted with caution.

Acknowledgments

This work was supported by the Natural Environment Research Council [NE/M01163/1]. This award is made under the auspices of the Environmental Microbiology and Human Health programme. This work represents the views of the results and the research and not the views of the funders. The comments from Darrel Baumgardner (Droplet Measurement Technologies) are gratefully acknowledged. The data will be available on 1ST July 2020 via the Environmental Information Data Centre, the Natural Environment Research Council's long-term data repository for terrestrial and freshwater sciences https://catalogue.ceh.ac.uk/eidc/documents.

Appendix A. Supplementary data

Supplementary data to this article can be found online at https://doi.org/10.1016/j.scitotenv.2018.08.120.

References

Anderson, B.D., Ma, M., Xia, Y., Wang, T., Shu, B., Lednicky, J.A., Ma, M.J., Lu, J., Gray, G.C., 2016. Bioaerosol sampling in modern agriculture: a novel approach for emerging pathogen surveillance? J. Infect. Dis. 214 (4), 537–545.

Bauer, H., Schueller, E., Weinke, G., Berger, A., Hitzenberger, R., Marr, I.L., Puxbaum, H., 2008. Significant contributions of fungal spores to the organic carbon and to the aerosol mass balance of the urban atmospheric aerosol. Atmos. Environ. 42 (22), 5542–5549.

Borlée, F., Yzermans, C.J., van Dijk, C.E., Heederik, D., Smit, L.A., 2015. Increased respiratory symptoms in COPD patients living in the vicinity of livestock farms. Eur. Respir. J. 46 (6), 1605–1614.

Bünger, J., Schappler-Scheele, B., Hilgers, R., Hallier, E., 2007. A 5-year follow-up study on respiratory disorders and lung function in workers exposed to organic dust from composting plants. Int. Arch. Occup. Environ. Health 80 (4), 306–312.

Crawford, I., Ruske, S., Topping, D.O., Gallagher, M.W., 2015. Evaluation of hierarchical agglomerative cluster analysis methods for discrimination of primary biological aerosol. Atmos. Meas. Tech. 8 (11), 4979.

Crawford, I., Lloyd, G., Herrmann, E., Hoyle, C.R., Bower, K.N., Connolly, P.J., Flynn, M.J., Kaye, P.H., Choularton, T.W., Gallagher, M.W., 2016. Observations of fluorescent aerosol–cloud interactions in the free troposphere at the High-Altitude Research Station Jungfraujoch. Atmos. Chem. Phys. 16 (4), 2273–2284.

van der Hoek, W., Morroy, G., Renders, N.H., Wever, P.C., Hermans, M.H., Leenders, A.C., Schneeberger, P.M., 2012. Epidemic Q fever in humans in the Netherlands. Adv. Exp. Med. Biol. 984, 329–364.

Douglas, P., Bakolis, I., Fecht, D., Pearson, C., Sanchez, M.L., Kinnersley, R., de Hoogh, K., Hansell, A.L., 2016. Respiratory hospital admission risk near large composting facilities. Int. J. Hyg. Environ. Health 219 (4–5), 372–379.

Gabey, A.M., Gallagher, M.W., Whitehead, J., Dorsey, J.R., Kaye, P.H., Stanley, W.R., 2010. Measurements and comparison of primary biological aerosol above and below a tropical forest canopy using a dual channel fluorescence spectrometer. Atmos. Chem. Phys. 10 (10), 4453–4466.

Gabey, A.M., Stanley, W.R., Gallagher, M.W., Kaye, P.H., 2011. The fluorescence properties of aerosol larger than 0.8 μm in urban and tropical rainforest locations. Atmos. Chem. Phys. 11 (11), 5491–5504.

Gabey, A.M., Vaitilingom, M., Freney, E., Boulon, J., Sellegri, K., Gallagher, M.W., Crawford, I.P., Robinson, N.H., Stanley, W.R., Kaye, P.H., 2013. Observations of fluorescent and biological aerosol at a high-altitude site in central France. Atmos. Chem. Phys. 13 (15), 7415–7428.

Hallar, A., Chirokova, G., McCubbin, I., Painter, T.H., Wiedinmyer, C., Dodson, C., 2011. Atmospheric bioaerosols transported via dust storms in the western United States. Geophys. Res. Lett. 38 (17).

Hernandez, M., Perring, A.E., McCabe, K., Kok, G., Granger, G., Baumgardner, D., 2016. Chamber catalogues of optical and fluorescent signatures distinguish bioaerosol classes. Atmos. Meas. Tech. 9 (7), 3283–3292.

Hill, S.C., Mayo, M.W., Chang, R.K., 2009. Fluorescence of Bacteria, Pollens, and Naturally Occurring Airborne Particles: Excitation/Emission Spectra (No. ARL-TR-4722). U.S. Army Research Lab, Adelphi.

Huffman, J.A., Treutlein, B., Pöschl, U., 2010. Fluorescent biological aerosol particle concentrations and size distributions measured with an ultraviolet aerodynamic particle sizer (UV-APS) in Central Europe. Atmos. Chem. Phys. 10 (7), 3215–3233.

Huffman, J.A., Sinha, B., Garland, R.M., Snee-Pollmann, A., Gunthe, S.S., Artaxo, P., Martin, S.T., Andreae, M.O., Pöschl, U., 2012. Size distributions and temporal variations of biological aerosol particles in the Amazon rainforest characterized by microscopy and real-time UV-APS fluorescence techniques during AMAZE-08. Atmos. Chem. Phys. 12 (24), 11997–12019.

Huffman, A., Prenni, J., DeMott, J., Pohlker, C., Mason, H., Robinson, H., Frohlich-Nowoisky, J., Tobo, Y., Despres, R., Garcia, E., Gochis, J., 2013. High concentrations of biological aerosol particles and ice nuclei during and after rain. Atmos. Chem. Phys. 13 (13), 6151–6164.

Jahne, M.A., Rogers, S.W., Holsen, T.M., Grimberg, S.J., Ramler, I.P., Kim, S., 2016. Bioaerosol deposition to food crops near manure application: quantitative microbial risk assessment. J. Environ. Qual. 45 (2), 666–674.

Kaye, P.H., Stanley, W.R., Hirst, E., Foot, E.V., Baxter, K.L., Barrington, S.J., 2005. Single particle multichannel bio-aerosol fluorescence sensor. Opt. Express 13 (10), 3583–3593.
Li, J., Zhou, L., Zhang, X., Xu, C., Dong, L., Yao, M., 2016. Bioaerosol emissions and detection of airborne antibiotic resistance genes from a wastewater treatment plant. Atmos. Environ. 124, 404–412.
Madsen, A.M., Thilsing, T., Bælum, J., Garde, A.H., Vogel, U., 2016. Occupational exposure levels of bioaerosol components are associated with serum levels of the acute phase protein Serum Amyloid A in greenhouse workers. Environ. Health 15 (1), 9.
Mazar, Y., Cytryn, E., Erel, Y., Rudich, Y., 2016. Effect of dust storms on the atmospheric microbiome in the Eastern Mediterranean. Environ. Sci. Technol. 50 (8), 4194–4202.
Morris, C.E., Leyronas, C., Nicot, P.C., 2014. Movement of bioaerosols in the atmosphere and the consequences for climate and microbial evolution. In: Colbeck, I., Lazaridis, M. (Eds.), Aerosol Science: Technology and Applications. John Wiley & Sons Ltd., pp. 393–415.
O'Connor, A.M., Auvermann, B., Bickett-Weddle, D., Kirkhorn, S., Sargeant, J.M., Ramirez, A., Von Essen, S.G., 2010. The association between proximity to animal feeding operations and community health: a systematic review. PLoS ONE 5 (3), e9530.
O'Connor, D.J., Healy, D.A., Hellebust, S., Buters, J.T., Sodeau, J.R., 2014. Using the WIBS-4 (Waveband Integrated Bioaerosol Sensor) technique for the on-line detection of pollen grains. Aerosol Sci. Technol. 48 (4), 341–349.
O'Connor, D.J., Daly, S.M., Sodeau, J.R., 2015. On-line monitoring of airborne bioaerosols released from a composting/green waste site. Waste Manag. 42, 23–30.
Pan, Y.L., 2015. Detection and characterization of biological and other organic-carbon aerosol particles in atmosphere using fluorescence. J. Quant. Spectrosc. Radiat. Transf. 150, 12–35.
Pan, Y.L., Hill, S.C., Pinnick, R.G., Huang, H., Bottiger, J.R., Chang, R.K., 2010. Fluorescence spectra of atmospheric aerosol particles measured using one or two excitation wavelengths: comparison of classification schemes employing different emission and scattering results. Opt. Express 18 (12), 12436–12457.
Pankhurst, L.J., Whitby, C., Pawlett, M., Larcombe, L.D., McKew, B., Deacon, L.J., Morgan, S.L., Villa, R., Drew, G.H., Tyrrel, S., Pollard, S.J., 2012. Temporal and spatial changes in the microbial bioaerosol communities in green-waste composting. FEMS Microbiol. Ecol. 79 (1), 229–239.
Pearce, D.A., Alekhina, I.A., Terauds, A., Wilmotte, A., Quesada, A., Edwards, A., Dommergue, A., Sattler, B., Adams, B.J., Magalhães, C., Chu, W.L., 2016. Aerobiology over Antarctica–a new initiative for atmospheric ecology. Front. Microbiol. 7, 16.
Pearson, C., Littlewood, E., Douglas, P., Robertson, S., Gant, T.W., Hansell, A.L., 2015. Exposures and health outcomes in relation to bioaerosol emissions from composting facilities: a systematic review of occupational and community studies. J. Toxicol. Environ. Health B 18 (1), 43–69.
Perring, A.E., Schwarz, J.P., Baumgardner, D., Hernandez, M.T., Spracklen, D.V., Heald, C.L., Gao, R.S., Kok, G., McMeeking, G.R., McQuaid, J.B., Fahey, D.W., 2015. Airborne observations of regional variation in fluorescent aerosol across the United States. J. Geophys. Res. Atmos. 120 (3), 1153–1170.
Pöhlker, C., Huffman, J.A., Pöschl, U., 2012. Autofluorescence of atmospheric bioaerosols–fluorescent biomolecules and potential interferences. Atmos. Meas. Tech. 5 (1), 37–71.
Robinson, N.H., Allan, J.D., Huffman, J.A., Kaye, P.H., Foot, V.E., Gallagher, M., 2013. Cluster analysis of WIBS single-particle bioaerosol data. Atmos. Meas. Tech. 6 (2), 337.
Roshchina, V.V., 2012. Vital autofluorescence: application to the study of plant living cells. Int. J. Spectrosc., 124672 https://doi.org/10.1155/2012/124672 (14 pages).
Saari, S., Niemi, J., Rönkkö, T., Kuuluvainen, H., Järvinen, A., Pirjola, L., Aurela, M., Hillamo, R., Keskinen, J., 2015. Seasonal and diurnal variations of fluorescent bioaerosol concentration and size distribution in the urban environment. Aerosol Air Qual. Res. 15 (2), 572–581.
Schumacher, C.J., Pöhlker, C., Aalto, P., Hiltunen, V., Petäjä, T., Kulmala, M., Pöschl, U., Huffman, J.A., 2013. Seasonal cycles of fluorescent biological aerosol particles in boreal and semi-arid forests of Finland and Colorado. Atmos. Chem. Phys. 13 (23), 11987–12001.
Sialve, B., Gales, A., Hamelin, J., Wery, N., Steyer, J.P., 2015. Bioaerosol emissions from open microalgal processes and their potential environmental impacts: what can be learned from natural and anthropogenic aquatic environments? Curr. Opin. Biotechnol. 33, 279–286.
Sun, J., Ariya, P.A., 2006. Atmospheric organic and bio-aerosols as cloud condensation nuclei (CCN): a review. Atmos. Environ. 40 (5), 795–820.
Sykes, P., Jones, K., Wildsmith, J.D., 2007. Managing the potential public health risks from bioaerosol liberation at commercial composting sites in the UK: an analysis of the evidence base. Resour. Conserv. Recycl. 52 (2), 410–424.
Taha, M.P.M., Pollard, S.J., Sarkar, U., Longhurst, P., 2005. Estimating fugitive bioaerosol releases from static compost windrows: feasibility of a portable wind tunnel approach. Waste Manag. 25 (4), 445–450.
Taha, M.P.M., Drew, G.H., Longhurst, P.J., Smith, R., Pollard, S.J., 2006. Bioaerosol releases from compost facilities: evaluating passive and active source terms at a green waste facility for improved risk assessments. Atmos. Environ. 40 (6), 1159–1169.
Taha, M.P.M., Drew, G.H., Vestlund, A.T., Aldred, D., Longhurst, P.J., Pollard, S.J., 2007. Enumerating actinomycetes in compost bioaerosols at source—use of soil compost agar to address plate 'masking'. Atmos. Environ. 41 (22), 4759–4765.
Toprak, E., Schnaiter, M., 2013. Fluorescent biological aerosol particles measured with the Waveband Integrated Bioaerosol Sensor WIBS-4: laboratory tests combined with a one year field study. Atmos. Chem. Phys. 13 (1), 225–243.
Vestlund, A.T., Al-Ashaab, R., Tyrrel, S.F., Longhurst, P.J., Pollard, S.J., Drew, G.H., 2014. Morphological classification of bioaerosols from composting using scanning electron microscopy. Waste Manag. 34 (7), 1101–1108.
Walser, S.M., Gerstner, D.G., Brenner, B., Bünger, J., Eikmann, T., Janssen, B., Kolb, S., Kolk, A., Nowak, D., Raulf, M., Sagunski, H., 2015. Evaluation of exposure–response relationships for health effects of microbial bioaerosols–a systematic review. Int. J. Hyg. Environ. Health 218 (7), 577–589.
Wei, K., Zou, Z., Zheng, Y., Li, J., Shen, F., Wu, C.Y., Yao, M., 2016. Ambient bioaerosol particle dynamics observed during haze and sunny days in Beijing. Sci. Total Environ. 550, 751–759.
Yu, X., Wang, Z., Zhang, M., Kuhn, U., Xie, Z., Cheng, Y., Pöschl, U., Su, H., 2016. Ambient measurement of fluorescent aerosol particles with a WIBS in the Yangtze River Delta of China: potential impacts of combustion-related aerosol particles. Atmos. Chem. Phys. 16 (17), 11337–11348.
Ziemba, L.D., Beyersdorf, A.J., Chen, G., Corr, C.A., Crumeyrolle, S.N., Diskin, G., Hudgins, C., Martin, R., Mikoviny, T., Moore, R., Shook, M., 2016. Airborne observations of bioaerosol over the Southeast United States using a wideband integrated bioaerosol sensor. J. Geophys. Res. Atmos. 121 (14), 8506–8524.